J Food Sci Technol (December 2019) 56(12):5194–5203
https://doi.org/10.1007/s13197-019-03988-z

ORIGINAL ARTICLE

Synthesis, characterization and cellular mineral absorption of nanoemulsions of *Rhododendron arboreum* flower extracts stabilized with gum arabic

Prince Chawla[1,4] · **Naveen Kumar**[2] · **Ravinder Kaushik**[1,5] · **Sanju B. Dhull**[3]

Revised: 16 June 2019 / Accepted: 26 July 2019 / Published online: 3 August 2019

Abstract To assess the cellular mineral uptake and oxidative stability of flower extract, a nanoscale gum arabic stabilized *Rhododendron arboreum* flower extract emulsion was formulated. Four different concentrations of flower extract (1–5%) were used for the optimization of the nanoemulsion. A significant ($P < 0.05$) difference was observed in average droplet size (43.51–55.87 nm) of the nanoemulsion. FTIR spectrum confirmed mainly C=C, aliphatic C–H, aliphatic and aromatic galacto-proteins, and polymeric-OH groups present in nanoemulsion. Smooth type of nanoemulsion was confirmed by inverted light microscopy. Ionic strength was evaluated and significant ($P < 0.05$) increase in particles size was attributed, whereas significant ($P < 0.05$) decrease in zeta potential was observed by increased NaCl concentration. Iron and calcium showed a non-significant difference in terms of mineral bioavailability. Calcium revealed significantly higher cellular uptake (52.11%) in comparison with iron (50.25%) and zinc (45.32%) during transwell assay. Higher cellular iron uptake unveiled a satisfactory amount of ferritin content

Keywords Gum arabic · Nanoemulsion · *Rhododendron arboreum* · TBA · Minerals · FTIR

Abbreviations

FE	Flower extract
NE	Nanoemulsion
DMEM	Dulbecco's modified eagles medium
PBS	Phosphate buffer saline
AAS	Atomic absorbance spectrophotometer
DLS	Dynamic light scattering
FTIR	Fourier transform infrared spectroscopy
TBA	Thiobarbituric acid

Introduction

Global population is gaining more interest in natural plant-based food products due to their potential health benefits and notable nutritional aspects (Ammar et al. 2015; Rachmawati et al. 2017). Since every part of a plant is valuable, numerous varieties of wild flowers such as Daylily, Mint, Chrysanthemum, Pansy, Rose, Tulip, Lilac and Rhododendron are widely used as functional ingredients for preparation of food, nutraceutical and medicinal products (Kiruba et al. 2011; Ammar et al. 2015; Popescu and Kopp 2017). Flowers improve the sensory characteristics such as appearance, taste and aesthetic values of foods, and aspects that consumers escalate justifying the growing trend of fresh top quality flowers' sales worldwide (Fernandes et al. 2018). Natural biodiversity of India is an emblem for the selection of natural foods for the human being. *Rhododendron* L. is one of the largest genera of

✉ Prince Chawla
princefoodtech@gmail.com

Naveen Kumar
nkft87@gmail.com

Ravinder Kaushik
ravinder_foodtech2007@rediffmail.com

Sanju B. Dhull
sanjudhull@gmail.com

[1] Shoolini University, Solan, Himachal Pradesh 173229, India

[2] Amity University, Jaipur, Rajasthan 303002, India

[3] Chaudhary Devi Lal University, Sirsa, Haryana 125055, India

[4] Lovely Professional University, Phagwara, Punjab 144411, India

[5] Amity University, Noida, Uttar Pradesh 201313, India

vascular plants that comprises 8 subgenera with more than 850 species and the majority of the species grow in the Himalayan region of India (Bhattacharyya 2011; Ranjitkar et al. 2014). Numerous researchers revealed hundreds of bioactive components in *Rhododendron* L. flowers that attribute various significant therapeutic and pharmacological importance (Louis et al. 2010; Qiang et al. 2011). These flowers are effectively used as anti-inflammatory, anti-nociceptive, antiprotozoal, antiviral, immunomodulatory, anti-diabetic, spasmolytic, sedative, acetylcholinesterase inhibitory, hepatoprotective, cardioprotective and anti-oxidants (García-Lafuente et al. 2009; Verma et al. 2010; Kim et al. 2011; Zhang et al. 2010; Gescher et al. 2011; Kumar et al. 2019). Several species of genus *Rhododendron* L. have been found in Himalayan region but *Rhododendron arboreum* is the most abundant. These flowers are traditionally used in the treatment of diarrhea, blood dysentery, high altitude sickness, headache, mental retardation, nasal bleeding, fever, and stomachache (Verma et al. 2010; Ranjitkar et al. 2014). In addition, due to numerous health benefits, there is substantial interest in the enrichment of food and beverage products with *Rhododendron arboreum* extracts (Pal and Bhattacharjee 2018). Furthermore, because of their mineral content, the food and beverage enrichment with *Rhododendron arboreum* extracts could be cost-effective, sustainable and optimal strategy against micronutrient human deficiencies (Gupta et al. 2015; Chawla et al. 2017; Pal and Bhattacharjee 2018). Nevertheless, numerous confronts are associated with the enrichment of these bioactive extracts into functional foods due to their chemical instability to oxygen, light, heat and anti-nutritional components of the food (Rachmawati et al. 2017). Therefore, to overcome the problem nanoemulsions stabilized and formulated with different plant-based biopolymers could be the potential and cost-effective approach (Ha et al. 2015; Taarji et al. 2018). These biopolymers conjugate effectively coat the bioactive compounds in the extracts, and prevent their chemical instability, ensuring their safe arrival in the target area. In this context, gum arabic is a widely used plant-based exudate gum for the preparation and stabilization of the oil in water nanoemulsion (Ha et al. 2015; Li et al. 2016; Taarji et al. 2018). However, no attempts have been made for the preparation and characterization of the gum arabic stabilized nanoemulsion of *Rhododendron arboreum* flower extract. Therefore, the aim of this study was to develop nanoemulsion of *Rhododendron arboreum* flower extract and to assess the in vitro bioavailability of minerals of flower extract through Caco-2 cell culture model. The objectives were as follows (i) Preparation and stabilization of the *Rhododendron arboreum* extract nano-emulsion, (ii) characterization of the respective emulsion, and (iii) assessment of in vitro mineral bioaccessibility of zinc, iron, calcium, and ferritin content of the nanoemulsion using transwell assay.

Materials and methods

Materials

Rhododendron arboreum flowers were obtained from the forest of the Solan, Himachal Pradesh, India. Gum arabic, tween 80, linoleic acid, α-amylase, lipase (human pancreatic), mucin, phospholipase, cholesterol esterase, pepsin, bovine serum albumin, pancreatin, glucosamine hydrochloride, glucuronic acid, ammonium sulphate, sodium salt hydrate of taurocholic acid were purchased from Sigma Aldrich Co. St. Louis, MO, USA. Phosphate buffer, sodium chloride, ethanol, L-ascorbic acid, calcium chloride were provided by Hi-Media Laboratories Pvt. Ltd., Mumbai, India. Caco-2 cells (Human colon adenocarcinoma) were obtained from National Centre for Cell Science, Pune, Maharashtra, India. DMEM (Dulbecco's Modified Eagles Medium), DMSO (dimethyl sulfoxide), Trypsin EDTA (0.25%), L-glutamine, phenol red and streptomycin (sulfate salt) were acquired from Sigma Aldrich, St. Louis, MO, USA; Human ferritin ELISA kit (SEA518Hu 96 Tests) from Cloud Clone-Corp. Houston, USA. Plastic dishes, plates, and transwell were obtained from Corning (Corning, NY, USA). Chemicals used were of AR grade. Triple distilled, cellular grade water and acid washed glassware were used throughout the experiments.

Methods

Preparation of ethanolic extract from Rhododendron arboretum flowers

Fresh RA were collected and taxonomical identification was confirmed in department of the botany, Shoolini University, Solan Himachal Pradesh, India. These fresh flowers were washed with tripled distilled water and petals were separated from the other parts of the flowers. Ethanolic extract of these flowers was prepared by following the method of Kiruba et al. (2011) and Gupta et al. (2015). Briefly, 20 g of fresh petals were dispersed into ethanol (1:5, w/v) and subjected for shaking using orbital shaker (Orbitek LT, Scigenics Biotech Pvt. Ltd., Chennai, India) for 48 h. Ethanolic extracts of flower was then filtered through Whatman no 1 filter paper. The extract was evaporated to dryness at refrigerated temperature (4–7 °C). The extracts were then stored in amber colored airtight containers at -20 °C until the further analysis.

Preparation of oil in water nanoemulsion

Nanoemulsion was prepared by following the method proposed by Li et al. (2016). Briefly, four different quantities of rhododendron flower extract (RE) (1, 2, 4, and 5 g) were dispersed into 10 ml of linoleic acid (LA) and completely dissolved using a magnetic stirrer (SPINOT MC 02, Tarsons Products Pvt. Ltd., Kolkata, India). Oil phase (RE + LA) was then mixed with 1% gum arabic solution (with 0.5% tween 80) using a magnetic stirrer. Probe sonicator (Sonics and Materials Inc. New Town, CT, USA) at 5 °C with 5.0 s pulse rate (20 min) was used for the formulation of final nanoemulsion samples (RE1NE, RE2NE, RE4NE, and RE5NE). Prepared samples were stored in glass vials at room temperature (25 °C) for further analysis.

Characterization of nanoemulsion

Droplet size distribution and zeta potential of the nanoemulsion Emulsion droplet size and zeta potential were determined at 25 °C using particle size and zeta potential analyzer (Zetasizer Nano ZS, Malvern Instruments Ltd. Malvern, WR14 1XZ, UK). For sample preparation, 1% emulsion sample was dissolved in triple distilled water and three measurements were acquired for each emulsion sample.

Fourier transform infrared (FTIR) spectroscopy FTIR spectrophotometer (Agilent Technologies, Mumbai, India) was used to evaluate functional groups of bioactive components and gum arabic present in nanoemulsion. Multiple scans of selected emulsion sample were accomplished against air in the mid-infrared region 4000–600 cm^{-1}. Data in terms of transmittance was obtained.

Microscopic evaluation of the nanoemulsion The microscopic and structural depiction of the nanoemulsion samples was scrutinized. All selected nanoemulsion samples were dispersed on the glass slide and sample was then covered with the coverslip. Selected nanoemulsion sample was evaluated under an inverted light microscope for the type of emulsion formed (400× magnification, Nikon digital sight, Japan).

Stability of the nano-emulsion

Ionic strength of the nanoemulsion Assessment of ionic strength of the nanoemulsion sample after 30 days of storage (30 °C) was evaluated using the method proposed by Li et al. (2016). Alteration in particle size and zeta potential confirmed the ionic strength of nanoemulsion after addition of final concentration of sodium chloride (0.5, 1 and 2 M).

TBA value of the nanoemulsion TBA value of nanoemulsion was assessed by following the method proposed by Sharma et al. (2017). Briefly, nanoemulsion (5 ml) sample was mixed with freshly prepared TBA (0.025 M, neutralized with sodium hydroxide and 2 M citric acid) reagent. The mixture of nanoemulsion and TBA reagent was heated instantly in boiling water bath (10 min). Additionally, 10 ml cyclohexanone and 1 ml of 4 M ammonium sulphate were added and the solution centrifuged at 5000 × *g* for 5 min at room temperature (30 °C). The orange-red cyclohexanone supernatant was collected and its absorbance was measured at 532 nm using UV–Visible spectrophotometer (Evolution 201, Thermo scientific, Mumbai, India).

Mineral estimation from nanoemulsion

Diverse trace elements (iron, zinc, calcium, copper), and sodium and potassium content of nanoemulsion were assessed in atomic absorption mode and in emission mode, respectively using AAS (AA-7000, Shimadzu, Tokyo, Japan) as described by Chawla et al. (2017).

In-vitro mineral bioavailability

A method defined by Sadh et al. (2017) was used to estimate the in vitro mineral bioavailability of trace elements of the selected nanoemulsion. Combination of simulated gastrointestinal and Caco-2 cell lines (transwell assay) were used for the evaluation of mineral bioavailability and cellular absorption, respectively.

Simulated gastrointestinal digestion For simulated gastrointestinal digestion, 5 ml of selected nanoemulsion was mixed with 1.92 ml saliva solution in a conical flask and the sample was incubated in an orbital shaker at 37 °C (95 rpm, 5 min). Further, gastric juice (2.9 ml) was mixed to the sample and pH 2 was adjusted using HCl and then incubated at 37 °C for 1 h. Duodenal juice (5.35 ml) and bile juice (1.92 ml) were mixed and incubated for 3 h. After centrifugation (REMI C24 Plus, REMI India) of samples using ultrafiltration centrifuge tube (Amicon, MW cutoff 10KDa) the percentage bioavailability of minerals was calculated as:

$$\text{Bioavailability}(\%) = \left(\frac{P}{C}\right) \times 100$$

where P = element concentration of dialysate, C = element concentration of sample.

Cellular absorption study (transwell assay) Caco-2 cells were cultured by following the method proposed by Sadh et al. (2017). For cell culturing antibiotic solution (Amphotericin 25 µg/ml, Streptomycin 30 µg/ml, Penicillin 100 µg/ml), fetal bovine serum (10%, heat inactivated), 2 mM L-Glutamine, and 1% DMEM were used as growth medium. Incubation of cells was attained in the CO_2 incubator (Thermo Fisher Scientific, Mumbai, India) at 37 °C in 95% humidified atmosphere with 5% CO2). Growth medium was changed on every alternate day and the passaging of cells was acquired at nearly 90% convergence, attained 7–8 days subsequently scattering a density of 1×10^6 cells/flasks. Trypsinization with 0.5% trypsin and 0.05% EDTA was accomplished for cell subculturing. Cells of 39 passaging was used for further mineral absorption assay. For cellular transference of iron zinc and calcium, a density of 50,000 cells/well were strewed into six welled plates (Sterile, 24 mm polyester membrane, pore size 0.4 µm) separating with an apical and basal portion. The cells were then endorsed to distinguish in the CO_2 incubator. Expended growth medium was pour out on every second day and washing of cells (three times) with PBS was also conducted. The monolayer became confluent subsequently 4–5 days and the cells were endorsed to discriminate for another 10 days before accomplishment transepithelial cellular absorption.

Valuation of cell monolayer integrity Structural characterization and presence of impurities were tested frequently using inverted light microscopy. After acquiring complete confluency the integrity of the Caco2 cells was also tested by the phenol red dye test. Following washing of cells, upper and lower chambers were filled with DMEM (2 ml) with phenol red dye and 2 ml PBS, respectively. After incubation, the 100 µl solution from upper and lower compartment was collected and the leakage of phenol red in the lower chamber was evaluated using automated ELISA plate reader (Epoch Bio Tek, Winooski, USA) at 558 nm.

Transport studies of minerals For transepithelial study of the minerals, formerly washed cells were loaded at the upper surface with 2 ml DMEM medium and mineral dialysate obtained after simulated gastrointestinal treatment (mineral concentration adjusted to 50 µM) into wells of plate. Similarly, 2 ml of DMEM was poured into the lower chamber and after incubation (37 °C, 3 h), the DMEM was aspirated off for evaluation of transepithelial absorption through cell line and the cells were further incubated for another 22 h for ferritin synthesis. Cellular transportation of minerals from both the chambers was examined using AAS.

Estimation of ferritin content

Human ferritin ELISA kit (DRG, GmbH, Germany) was used for evaluation of intracellular ferritin formation in the cell line. Washed cells (with PBS) were garnered with trypsinization and collected cells were mixed with 2 ml of cellular grade water and cell lysis was acquired with probe sonicator at 4 °C for 2 min with a pulse rate of 5 s. Ferritin content was estimated according process described in ferritin kit.

Statistical analysis

Microsoft excel, 2016 (Microsoft Corp., Redmond, WA) was used for the calculation of standard error mean (SEM). Statistical difference in terms of significant and non-significant values was confirmed by one way and two-way analysis of variance and comparison between means was completed by critical difference value (Kaushik et al. 2015).

Results and discussion

Optimization and physicochemical characteristics of nanoemulsion

An effective emulsion system transmits both aqueous and the oil phase, hence linoleic acid was used as an oil phase for proper immersion of rhododendron extract (RE). For optimization of suitable nanoemulsion system amount of emulsifier, surfactant and LA were kept a constant and different amount of RE were used for the formulation of RE1NE, RE2NE, RE4NE, and RE5NE. Stability of an emulsion system is an important factor for significant food and pharmacological applications, therefore all the samples were evaluated for thermal stability against amalgamation and flocculation at 30 °C for 15 days. After storage, none of the emulsion samples exhibited amalgamation and a possible reason for this could be the transformation of ultrasound waves through an aqueous medium, which formed implosive breakdown of microbubbles. This ephemeral collapse situation created a localized hot spot region that ultimately resulted in minute droplets in the emulsion system (Carpenter and Saharan 2017). Droplet size and zeta potential of all nanoemulsion samples were measured and results of droplet size are depicted in Fig. 1a. Droplet size of the nanoemulsion samples was ranged from 43.51 to 55.87 nm. All the nanoemulsion showed significant ($P < 0.05$) difference in droplet size with increasing concentration of RE. Campelo et al. (2017) evaluated the stabilization of emulsion of gum arabic and whey protein isolate and observed a slight increase in droplet size as oil

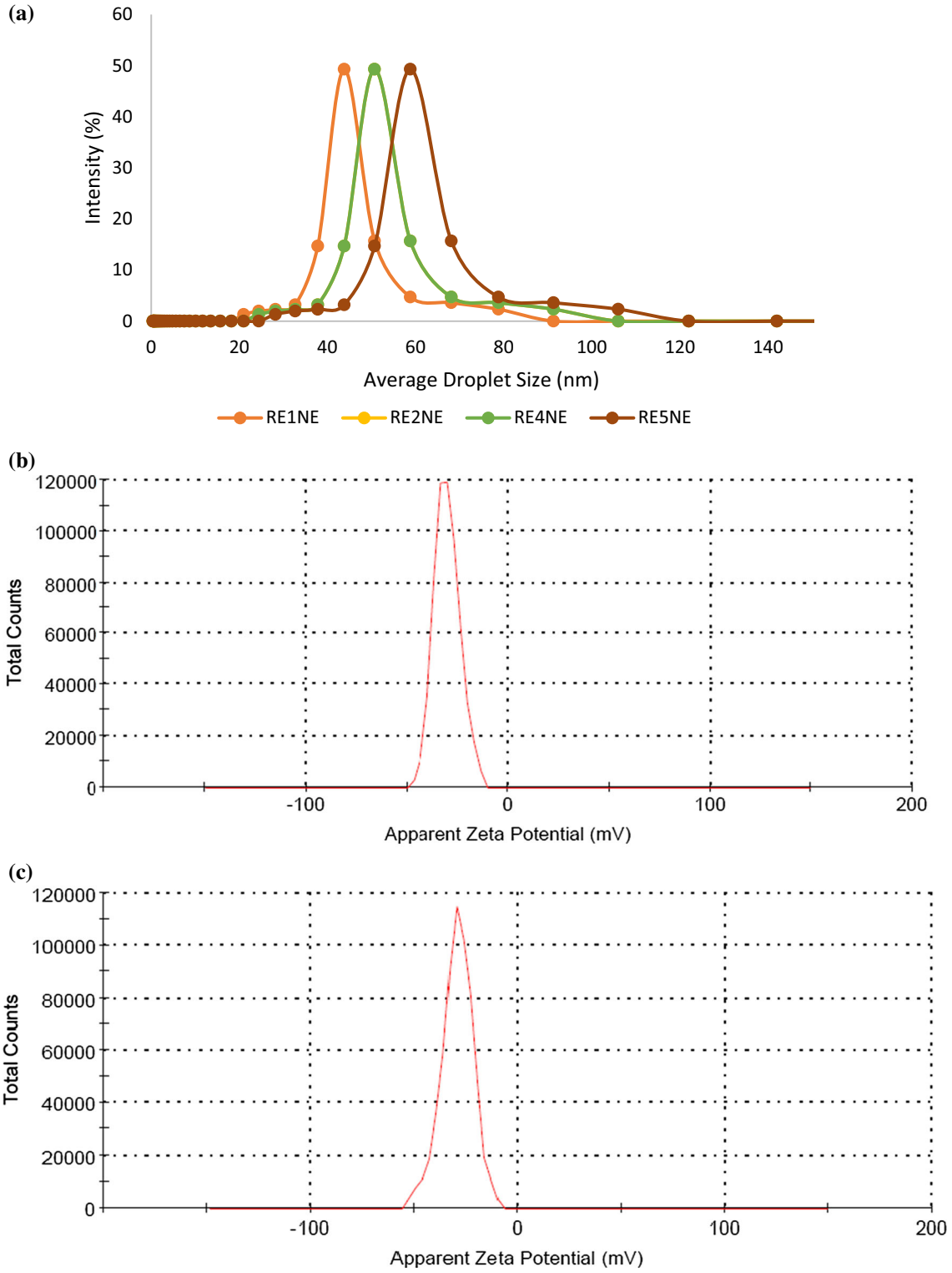

Fig. 1 **a** Average particle size of RE1NE, RE2NE, RE4NE, RE5NE nanoemulsion and Zeta potential of **b** RE1NE, **c** RE2NE, **d** RE4NE, and **e** RE5NE nanoemulsion

concentration increasing. Electrostatic contribution to the mechanism by which gum arabic stabilized the nanoemulsion was assessed by zeta potential of the nanoemulsion and results are depicted in Fig. 1b–e. Non-significant ($P < 0.05$) difference was observed in zeta potential values of all the nanoemulsion samples,

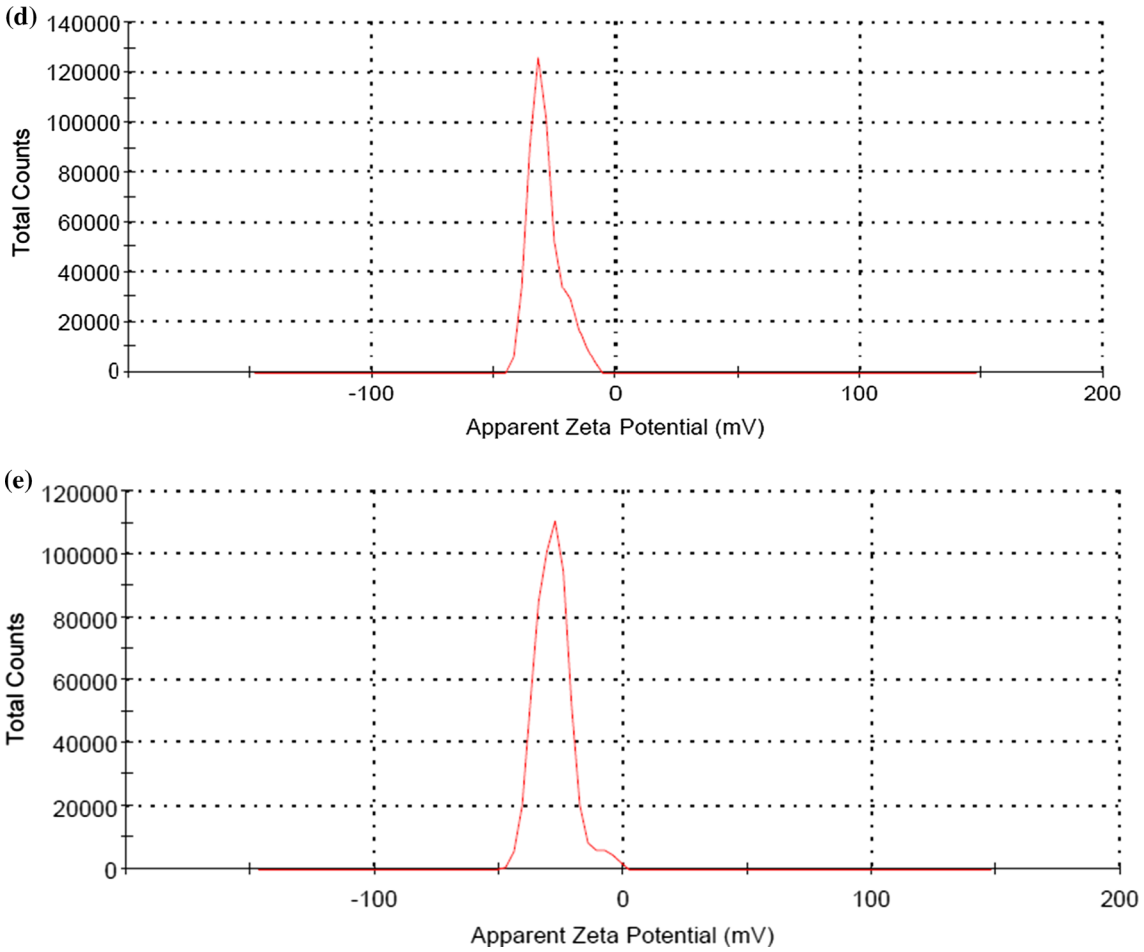

Fig. 1 continued

respectively. Negative charge potential distribution on nanoemulsion could be due to the highly anionic behavior of gum arabic and least molecular weight of the nonionic surfactant. Gum arabic also specified itself correlate with a non-ionic surfactant and continuous phase through hydrophobic binding capability and ionic interaction. In addition, the negative charge on nanoemulsion system was attributed due to interfacing of arabino-galacto proteins of gum arabic with polysaccharide moieties that extended into the aqueous solution to give rise to a steric stabilizing layer (Jayme et al. 1999). However, all the nanoemulsion samples did not show any variation in terms of particle size and zeta potential, hence nanoemulsion with the highest concentration of RE was selected for further analysis.

FTIR and optical properties of nanoemulsion

The result of the FTIR spectrum for nanoemulsion is depicted in Fig. 2a. When molecules of gum arabic affixed with surfactant and oil phase the stretching, frequencies originating from the functional groups of the gum arabic were predictable to shift consequently. Herein, a huge peak at 3339 cm^{-1}.confirmed the vibrational stretching of the polymeric–OH group of the nanoemulsion which was mainly attributed by the water phase and phenolic groups of FE present in the nanoemulsion. Furthermore, vibrational characteristics of C–H aliphatic stretch was shifted at 2422 cm^{-1}, which could be due to the presence of nonionic surfactant associated with nanoemulsion system. Confirmation of aliphatic and aromatic galacto-proteins and prevalence of amino acids in the nanoemulsion sample was also confirmed at 1700–1640 cm^{-1}. Vibrational bands between 2273 and 1927 cm^{-1} were attributed by fatty acids and galacto-proteins. Moreover, C=C stretching also confirmed at 1640 cm-1 which could be due to the presence of carboxylic moiety of gum arabic.

Surface characterization and morphological behavior of RE5NE was assessed by inverted light microscopy and the result is shown in Fig. 2b. Results of inverted light microscopy definite the smooth type of nanoemulsion, however, few numbers of emulsion droplets appeared which could disclose the stabilization of colloidal system

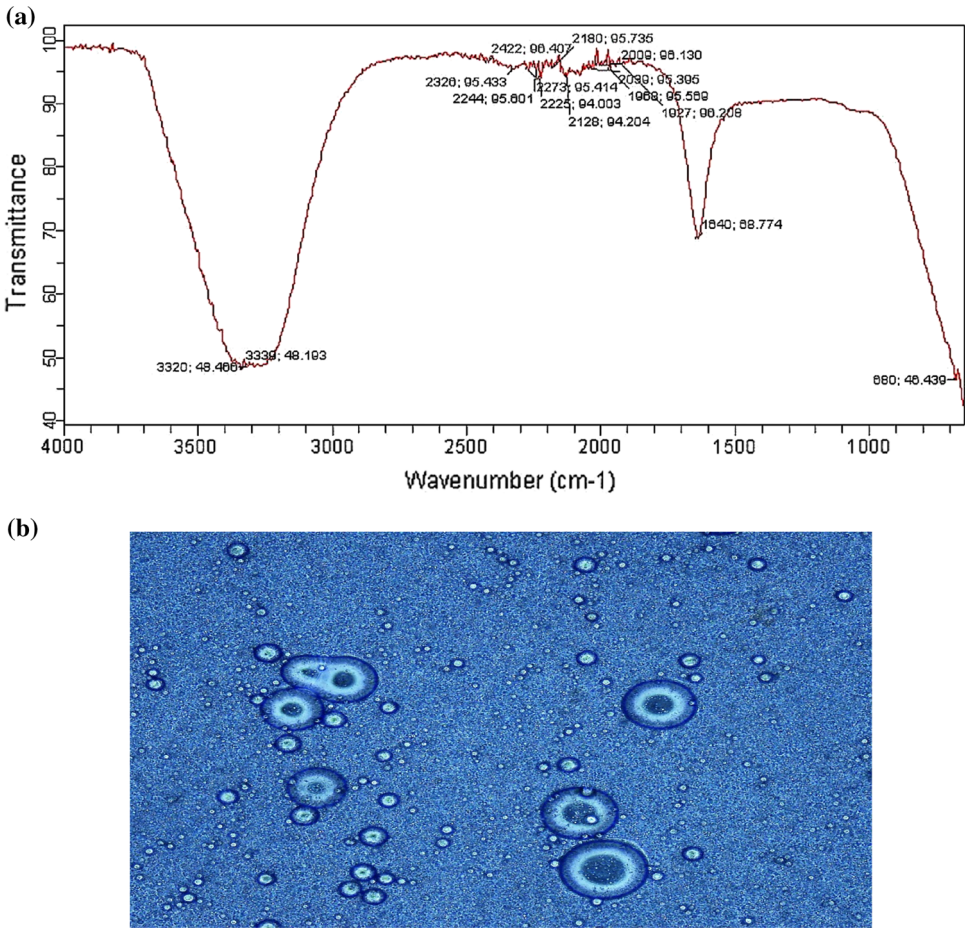

Fig. 2 **a** ATR-FTIR spectrum and **b** smooth type inverted light microscope image of freshly prepared RE5NE nanoemulsion

of the nanoemulsion. Smooth type of emulsion could be due to adherence of oil droplets with the emulsifier and electrostatic stability due to repulsion among droplets and high surface charge of the gum arabic (Sari et al. 2015).

Ionic strength and oxidative stability of the nanoemulsion

Stability of nanoemulsion always influenced by the salt concentration and it is expected that with increasing concentration of salt strength of nanoemulsion should be suitable. For evaluation of the ionic strength of RE5NE, nanoemulsion different concentrations of sodium chloride were used and results are illustrated in (Table 1). Ionic strength was evaluated by observing the droplet size and zeta potential of the nanoemulsion. Results shown significant ($P < 0.05$) increase in droplet size on 0 day with cumulative salt concentration and a similar trend was observed on 30th day of storage. Increase in droplet size of nanoemulsion with increasing salt concentration could be due to the presence of negatively charged carboxylate group which exhibit electrostatic interaction with positively charged sodium ions (Li et al. 2016).

Similarly, the electrostatic attraction also inclined zeta potential of the nanoemulsion and resulted in significant ($P < 0.05$) decrease in zeta potential value with increasing ionic strength on 0 and 30th day of storage, respectively. Despite poly-anionic nature gum arabic also consist of slightly positive charge and flower extract also consist of positive charge which could be the possible reason for decreased zeta potential of nanoemulsion on 0 as well as the 30th day of storage. This positive charge and negatively charged chloride ions slightly influence the electrostatic repelling force. In addition of decreased zeta potential and increased particle size it also concluded that nanoemulsion exhibited colloidal stability because no sign of coalescence and flocculation were visible (Li et al. 2016). Results were in accord with the finding of Guan et al. (2016) who revealed a significant increase in particle size and a decrease in zeta potential value of whey protein, lecithin and tween 80 stabilized nanoemulsion during the analysis of the ionic strength of the nanoemulsion.

Disruption in an emulsion system due to gravitational or centrifugal forces and upward accumulation of oil droplets leads to oxidative deterioration. To evaluate the oxidative stability of selected nanoemulsion TBA value was

Table 1 Impact of ionic strength on droplet size and zeta potential of RE5NE nanoemulsion stored at room temperature (30 °C)

Concentration of NaCl solution	Particle size (nm) 0 day	Particle size (nm) 30th day	Zeta potential (mV) 0 day	Zeta potential (mV) 30th day
0.5 M NaCl	55.87 ± 1.13^{a}	58.16 ± 1.14^{b}	-35.22 ± 0.08^{b}	-36.87 ± 0.05^{a}
1.0 M NaCl	56.39 ± 1.35^{a}	60.23 ± 1.29^{b}	-22.39 ± 0.02^{b}	-23.42 ± 0.06^{a}
2.0 M NaCl	57.71 ± 1.06^{a}	63.42 ± 1.83^{b}	-18.37 ± 0.07^{b}	-19.76 ± 0.03^{a}

Data are presented as mean ± SEM (n = 3)

[a,b]Means within row with different lowercase superscript are significantly different ($p < 0.05$) from each other

calculated during storage of the 7 days (30 °C). Linoleic acid is a highly unsaturated fatty acid and is more susceptible to oxidative deterioration, therefore TBA values of both linoleic acid and RE5NE was calculated and results are shown in Table 2. Both linoleic acid and RE5NE were kept in an open vial at 30 °C for the oxidation process. Results revealed significant ($P < 0.05$) difference in TBA value of both linoleic acid and RE5NE up to 7 days of storage. Linoleic acid showed significant ($P < 0.05$) increase in TBA value (from 0.08 to 0.87) as increasing days of storage, and RE5NE showed non-significant ($P < 0.05$) difference in TBA value during storage. Gum arabic and flower extract attributed antioxidant stability against heat and oxygen during storage but linoleic acid produced malondialdehyde (main marker in lipid peroxidation) and thiobarbituric acid reacted with malondialdehyde, which resulted in significantly higher TBA value.

Mineral content and in vitro mineral bioavailability

The result of mineral content is presented in (Table 3) and results shown significant ($P < 0.05$) difference in all the minerals of the selected nanoemulsion. Sodium content (444.64 ppm) was significantly ($P < 0.05$) higher, whereas copper content (11.19 ppm) was least in amount as compared to other minerals present in the selected emulsion. Iron, zinc, and calcium are essential minerals, therefore in vitro mineral bioavailability of iron, zinc, and calcium of RE5NE was evaluated. For simulated gastrointestinal selected nanoemulsion sample was subjected for different enzyme treatments and results of in vitro mineral bioavailability are illustrated in (Fig. 3). Results of mineral bioavailability unveiled non-significant ($P < 0.05$) difference in percentage bioavailability of iron and calcium, whereas zinc exhibited significant ($P < 0.05$)

Table 2 TBA value of linoleic acid and RE5NE nanoemulsion stored at room temperature (30 °C)

Sample → duration↓	TBA value at room temperature (30 °C)	
	Linoleic acid	RE5NE
0 day	0.08 ± 0.001^{aB}	0.00 ± 0.000^{aA}
3rd day	0.29 ± 0.003^{bB}	0.01 ± 0.001^{aA}
5th day	0.61 ± 0.004^{cB}	0.02 ± 0.001^{aA}
7th day	0.87 ± 0.003^{dB}	0.02 ± 0.002^{aA}

Data are presented as mean ± SEM (n = 3)

[a–d]Means within column with different lowercase superscript are significantly different ($p < 0.05$) from each other

[A,B]Means within row with different upper superscript are significantly different ($p < 0.05$) from each other

Table 3 Mineral content of RE5NE nanoemulsion

Minerals	RE5NE nanoemulsion (PPM)
Iron	58.19 ± 1.29^{c}
Zinc	39.45 ± 1.49^{b}
Copper	11.19 ± 1.85^{a}
Calcium	171.10 ± 2.97^{d}
Sodium	444.64 ± 5.52^{f}
Potassium	112.45 ± 1.36^{e}

Data are presented as mean ± SEM (n = 3)

[a–e]Means within row with different lowercase superscript are significantly different ($p < 0.05$) from each other

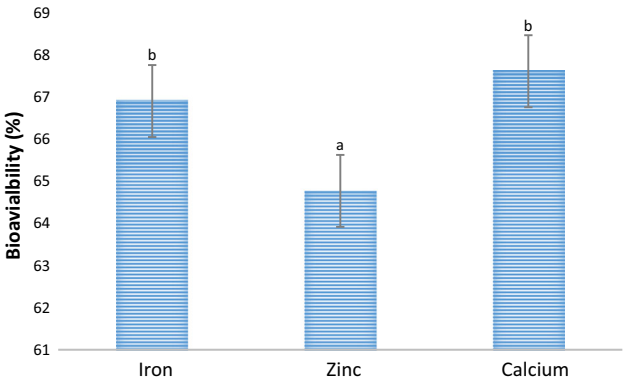

Fig. 3 Mineral bioavailability of RE5NE nanoemulsion. Data are presented as mean ± SEM (n = 3). [a,b]Means within column with different lowercase superscript are significantly different ($p < 0.05$) from each other

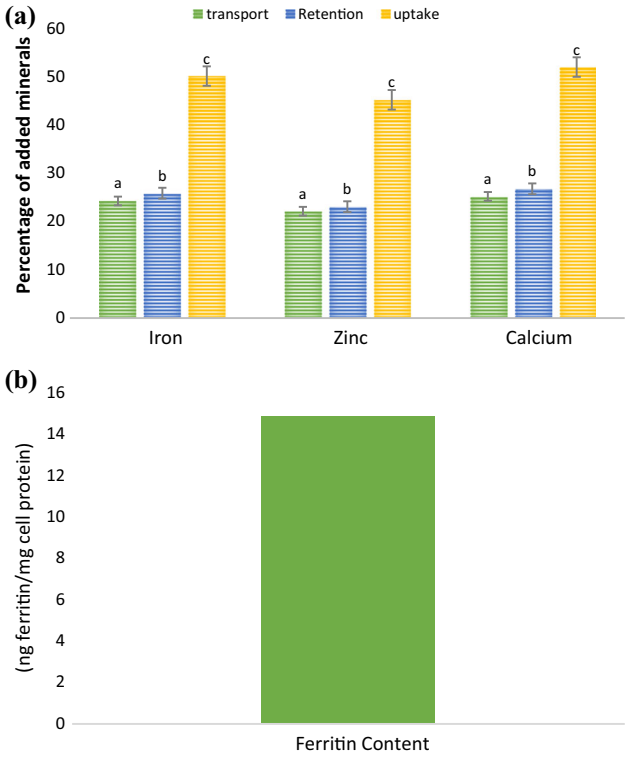

Fig. 4 **a** Iron, zinc, and calcium transport, retention and uptake* through Caco-2 cells from RE5NE nanoemulsion and **b** Ferritin synthesis in Caco-2 cells from RE5NE nanoemulsion. Data are presented as mean ± SEM (n = 3). [a,c]Means within column with different lowercase superscript are significantly different ($p < 0.05$) from each other. *uptake = transport plus retention

difference in terms of mineral bioavailability. From our findings, it can be concluded that gum arabic and nonionic surfactant shielded flower extract in high acidic condition and flower extract revealed suitable mineral bioavailability. For cellular absorption of minerals, digested samples obtained after simulated gastrointestinal digestion were subjected for transwell assay. For cellular uptake and transport of minerals, 50 µM concentration of iron, zinc, and calcium was loaded on Caco-2 cells (apical chamber of transwell plate) and results are depicted in (Fig. 4a). From the results, it could be concluded that RE5NE exhibited significant ($P < 0.05$) difference in transport retention and uptake of the iron, zinc, and calcium respectively. However, calcium showed significantly ($P < 0.05$) higher transport (25.27%), retention (26.84%), and uptake (52.11%) in comparison with iron and zinc. Higher cellular uptake of calcium could be due to the maximum binding of calcium with cellular proteins (Chawla et al. 2017; Gupta et al. 2015). Furthermore, ferritin content was evaluated to signify the storage form of the iron present in the cells after the addition of the RE5NE. Cellular iron uptake expressed as a ratio of ferritin and cell protein (ng ferritin/mg cell protein) (Fig. 4b). During cellular transportation, iron showed a 50.25% uptake of the added iron that resulted in the synthesis of 14.87 ng ferritin/mg cell protein. Higher ferritin content was attributed mainly due to the presence of higher cellular protein (Sharma et al. 2017).

Conclusion

A nanoscale gum arabic stabilized *RA* nanoemulsion with a significantly lower average droplet size and high zeta potential was effectively formulated. Optimized nanoemulsion exhibited a smooth type of morphology and enduring oxidative stability that suitable for pharmaceutical applications and delivery of hydrophobic components. Ionic strength was explored by adding sodium chloride solution and significant ($P < 0.05$) increase in particle size was observed with increased ionic concentration. Iron and calcium showed non-significant ($P < 0.05$) difference in terms of mineral bioavailability, however, calcium showed significantly ($P < 0.05$) higher cellular uptake during transwell assay. Higher cellular iron uptake confirmed the synthesis of efficient ferritin content. In conclusion, this investigation formulated a simple, reproducible and cost-effective nanoemulsion that has remarkable potential for emerging functional foods and enteral nutrition with effective storage and oxidative stability. Additionally, this nanoemulsion system also embraces potential as a conveyance system to encapsulate and protect micronutrients, bioactive compounds, and drugs.

Acknowledgements The support by School of Bioengineering and Food Technology, Shoolini University, Solan, Himachal Pradesh, India is gratefully acknowledged.

References

Ammar I, Ennouri M, Attia H (2015) Phenolic content and antioxidant activity of cactus (*Opuntia ficus-indica* L.) flowers are modified according to the extraction method. Ind Crop Product 64:97–104

Bhattacharyya D (2011) Rhododendron species and their uses with special reference to Himalayas—a review. Assam Uni J of Sci Tech 7(1):161–167

Campelo PH, Junqueira LA, Resende JVD, Zacarias RD, Fernandes RVDB, Botrel DA, Borges SV (2017) Stability of lime essential oil emulsion prepared using biopolymers and ultrasound treatment. Int J Food Prop 20(1):S564–S579

Carpenter J, Saharan VK (2017) Ultrasonic assisted formation and stability of mustard oil in water nanoemulsion: effect of process parameters and their optimization. Ultrason Sonochem 35:422–430

Chawla P, Bhandari L, Sadh PK, Kaushik R (2017) Impact of solid-state fermentation (*Aspergillus oryzae*) on functional properties and mineral bioavailability of black-eyed pea (*Vigna unguiculata*) seed flour. Cereal Chem 94(3):437–442

Fernandes L, Saraiva JA, Pereira JA, Casal S, Ramalhosa E (2018) Post-harvest technologies applied to edible flowers: a review: edible flowers preservation. Food Rev Int 32:1–23

García-Lafuente A, Guillamón E, Villares A, Rostagno MA, Martínez JA (2009) Flavonoids as anti-inflammatory agents: implications in cancer and cardiovascular disease. Inflamm Res 58(9):537–552

Gescher K, Kühn J, Hafezi W, Louis A, Derksen A, Deters A, Hensel A (2011) Inhibition of viral adsorption and penetration by an aqueous extract from *Rhododendron ferrugineum* L. as antiviral principle against herpes simplex virus type-1. Fitoterapia 82(3):408–413

Guan Y, Wu J, Zhong Q (2016) Eugenol improves physical and chemical stabilities of nanoemulsions loaded with β-carotene. Food Chem 194:787–796

Gupta C, Chawla P, Arora S, Tomar SK, Singh AK (2015) Iron microencapsulation with blend of gum arabic, maltodextrin and modified starch using modified solvent evaporation method–milk fortification. Food Hydrocoll 43:622–628

Ha TVA, Kim S, Choi Y, Kwak HS, Lee SJ, Wen J, Ko S (2015) Antioxidant activity and bioaccessibility of size-different nanoemulsions for lycopene-enriched tomato extract. Food Chem 178:115–121

Jayme ML, Dunstan DE, Gee ML (1999) Zeta potentials of gum arabic stabilised oil in water emulsions. Food Hydrocoll 13(6):459–465

Kaushik R, Sachdeva B, Arora S (2015) Heat stability and thermal properties of calcium fortified milk. Cyta J Food 13(2):305–311

Kim SJ, Um JY, Hong SH, Lee JY (2011) Anti-inflammatory activity of hyperoside through the suppression of nuclear factor-κB activation in mouse peritoneal macrophages. Am J Chin Med 39(01):171–181

Kiruba S, Mahesh M, Nisha SR, Paul ZM, Jeeva S (2011) Phytochemical analysis of the flower extracts of RA Sm. ssp. nilagiricum (Zenker) Tagg. Asian Pac J Trop Biomed 1(2):284–286

Kumar V, Suri S, Prasad R, Gat Y, Sangma C, Jakhu H, Sharma M (2019) Bioactive compounds, health benefits and utilization of Rhododendron: a comprehensive review. Agri Food Security 8(1):6

Li J, Hwang IC, Chen X, Park HJ (2016) Effects of chitosan coating on curcumin loaded nano-emulsion: study on stability and in vitro digestibility. Food Hydrocoll 60:138–147

Louis A, Petereit F, Lechtenberg M, Deters A, Hensel A (2010) Introduction. Planta Med 76:1550–1557

Pal S, Bhattacharjee P (2018) Spray dried powder of lutein-rich supercritical carbon dioxide extract of gamma-irradiated marigold flowers: process optimization, characterization and food application. Powder Tech 327:512–523

Popescu R, Kopp B (2017) The genus Rhododendron: an ethnopharmacological and toxicological review. J Ethnopharma 147(1):42–62

Qiang Y, Zhou B, Gao K (2011) Chemical constituents of plants from the genus Rhododendron. Chem Biodiv 8(5):792–815

Rachmawati H, Novel MA, Nisa RM, Berlian G, Tandrasasmita OM, Rahma A, Tjandrawinata RR (2017) Co-delivery of curcumin-loaded nanoemulsion and Phaleria macrocarpa extract to NIH 3T3 cell for antifibrosis. J Drug Delivery Sci Tech 39:123–130

Ranjitkar S, Kindt R, Sujakhu NM, Hart R, Guo W, Yang X, Luedeling E (2014) Separation of the bioclimatic spaces of Himalayan tree rhododendron species predicted by ensemble suitability models. Glob Eco Conserv 1:2–12

Sadh PK, Chawla P, Bhandari L, Kaushik R, Duhan JS (2017) In vitro assessment of bio-augmented minerals from peanut oil cakes fermented by *Aspergillus oryzae* through Caco-2 cells. J food Sci Tech 54(11):3640–3649

Sari TP, Mann B, Kumar R, Singh RRB, Sharma R, Bhardwaj M, Athira S (2015) Preparation and characterization of nanoemulsion encapsulating curcumin. Food Hydrocoll 43:540–546

Sharma A, Shree BS, Arora S, Kapila S (2017) Preparation of lactose-iron complex and its cyto-toxicity, in vitro digestion and bioaccessibility in Caco-2 cell model system. Food Bioscience 20:125–130

Taarji N, da Silva CAR, Khalid N, Gadhi C, Hafidi A, Kobayashi I, Nakajima M (2018) Formulation and stabilization of oil-in-water nanoemulsions using a saponins-rich extract from argan oil press-cake. Food Chem 246:457–463

Verma N, Singh AP, Amresh G, Sahu PK, Rao CV (2010) Anti-inflammatory and anti-nociceptive activity of RA. J Pharm Res 3:1376–1380

Zhang XN, Li JM, Yang Q, Feng B, Liu SB, Xu ZH, Guo YY, Zhao MG (2010) Anti-apoptotic effects of hyperoside via inhibition of NR2B-containing NMDA receptors. Pharmacological reports 62(5):949–955